JOURNAL OF GEOPHYSICAL RESEARCH, VOL. 102, NO. D19, PAGES 23,269-23,275, OCTOBER 20, 1997

Thermodynamic and optical properties of sea salt aerosols

I. N. Tang, A. C. Tridico[1], and K. H. Fung

Brookhaven National Laboratory, Department of Applied Science, Environmental Chemistry Division
Upton, New York

Abstract. Sea salt particles are constantly produced from ocean surfaces by wave-wind interactions and removed by deposition and precipitation scavenging. These particles constitute the background aerosol for light scattering in the marine boundary layer. In this work, the thermodynamic and optical properties of sea salt aerosol particles generated from seawater samples are measured at 25°C as a function of relative humidity, using a single-particle levitation technique. Water activities, densities, and refractive indices of aqueous solution droplets containing a single salt NaCl, Na_2SO_4, $MgCl_2$, or $MgSO_4$ are also reported as a function of concentration. The light-scattering properties of the sea salt aerosol are modeled by the external mixture of these four salt systems selected to approximate the sea salt composition. Good agreements are obtained. It follows that in either visibility reduction or radiative forcing calculations, both freshly produced and aged sea salt aerosols may be modeled by external mixtures of the appropriate inorganic salts, whose solution properties are now available in the literature.

1. Introduction

Aerosols play an important role in the Earth's climate through their direct and indirect interactions with solar radiation [*Charlson et al.*, 1991, 1992; *Kiehl and Briegleb*, 1993]. Recently, much attention has been given to the behavior of sulfate and nitrate aerosols because of their increasing abundance in the atmosphere due to anthropogenic emissions. In contrast, little is known about the thermodynamic and optical properties of sea salt particles, which are constantly produced by wave-wind interactions on ocean surfaces. These particles are known to form background aerosols for light scattering in the marine boundary layer [*Fitzgerald*, 1991]. The chemical composition of the sea salt aerosol, however, is complex and can vary with time and location. For example, the elemental ratios of Cl, Na, and S observed in many sea salt aerosol particles differ from those in the normal seawater [*McInnes et al.*, 1994]. Reactions of sea salt particles with sulfuric and nitric acid in the atmosphere are expected to release HCl gas, leaving behind particles with reduced Cl/Na ratio and enriched sulfate and nitrate contents. Chloride deficits in sea salt particles may also be caused by reactions with gaseous nitrogen oxides [*Duce*, 1969; *Finlayson-Pitts et al.*, 1989] or by oxidation of dissolved SO_2 by O_3 [*Chameides and Stelson*, 1992]. Therefore the chemical composition can be quite different between freshly produced and aged sea salt particles.

Sea salt particles are hygroscopic by nature. They deliquesce to become aqueous solution droplets when the relative humidity (RH) rises in the atmosphere. Once in solution, a droplet will continue to absorb water and grow in size and weight as RH increases further. As RH gradually decreases, the solution droplet will lose water by evaporation but will remain a metastable solution supersaturated with solutes until it finally effloresces at low enough RH and returns to a solid particle. Such hysteresis behavior, not found in bulk solutions, is in fact common to hygroscopic aerosol particles [*Orr et al.*,1958; *Tang*, 1976]. Consequently, modeling of atmospheric aerosols including sea salt particles requires extensive water activity, density, and refractive index data inaccessible to measurement with bulk solutions.

In this paper, measurements of the thermodynamic and optical properties of sea salt particles are made at 25°C as a function of RH, using the single-particle levitation technique developed for droplet evaporation studies. Water activities, densities, and refractive indices of solution droplets containing a single salt NaCl, Na_2SO_4, $MgCl_2$, or $MgSO_4$ are also reported as a function of concentration. The data reported here provide an opportunity to further test the external mixture concept [*Tang*, 1996, 1997] for predicting the light-scattering properties of mixed-salt aerosols as complex as the sea salt particles.

2. Experimental Procedure

The apparatus and experimental procedures have been described in detail previously [*Tang and Munkelwitz*, 1994a]. Briefly, a charged salt particle, 6-8 μm in diameter, is suspended in a quadrupole cell (or called an electrodynamic balance) under the illumination of a He-Ne laser light. The cell is first evacuated and then back-filled with water vapor under

[1]Now at Finnegan, Henderson, Farabow, Garrett & Dunner, 1300 Eye Street, N.W., Washington, DC 20005.

Paper number 97JD01806.
0148-0227/97/97JD-01806$09.00

controlled conditions for the particle to deliquesce and grow into a droplet by water vapor condensation. Droplet evaporation takes place when the cell is once again slowly evacuated of its water vapor. The droplet weight changes during growth and evaporation are continuously measured by the dc voltages required to balance the particle against gravity. At the same time, the droplet size changes are continuously monitored by its 90° scattered light.

Reagent grade chemicals were used without further purification. The sea salt particles were generated from filtered seawater samples. The Long Island seawater sample was collected at the shores of Long Island Sound in New York. The offshore ocean water sample was obtained from the Atlantic Ocean several miles off the coast of Long Island.

3. Results and Discussion

3.1. Hydration Behavior

The phase transformation, growth, and evaporation processes described above for hygroscopic particles are illustrated in Figure 1 for a sea salt particle generated from the Atlantic Ocean seawater sample. Here, the particle mass change with respect to the dry salt mass, w/w_0, is plotted as a function of RH. As a comparison, the hydration behavior of a pure NaCl particle is also shown in Figure 1 as the dashed lines. Upon increasing RH, while a solid NaCl particle remains unchanged in weight until it deliquesces at 75.3% RH, the sea salt particle is seen to absorb water gradually all the way up to about 70% RH, where it rapidly picks up more water to become a homogeneous solution droplet at about 74% RH. Both droplets then grow continuously and smoothly as RH is further increased. As RH decreases, each droplet gradually loses its mass by water evaporation but remains a metastable solution until efflorescence occurs at about 45-48% RH, which is much lower than its deliquescence point. However, unlike the NaCl particle, which sheds all its water content upon crystallization, the sea salt particle does not return to the initial weight immediately. In fact, there is always some residual water remaining in sea salt particles even after pumping in the vacuum at 10^{-6} torr.

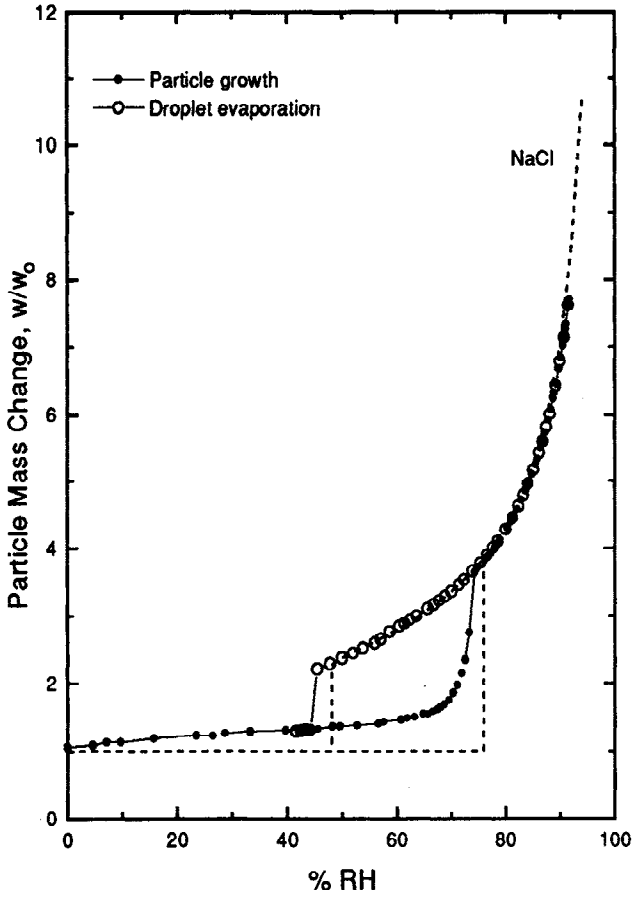

Figure 1. Phase transformation, growth, and evaporation of a sea salt particle as a function of relative humidity. For comparison, the hydration behavior of a pure NaCl particle is illustrated as dashed curves and lines.

Sea salt is a complex mixture of inorganic salts and may also contain organic compounds as minor components. The elemental composition of the "standard seawater" can be found in various references and handbooks [e.g., *Sverdrup et al.*, 1942]. The relative concentrations of the major ions in the standard seawater are given in Table 1, where Na^+ is taken as the reference species. We have previously studied the properties and behavior of mixed-salt aerosols [*Tang*, 1976; *Tang and Munkelwitz*, 1994b] . The hydration behavior of a mixed-salt particle is more complicated in that after it has first deliquesced, it may go through partially dissolved states before finally becoming a homogeneous solution droplet. The observed hydration behavior of sea salt particles, as illustrated in Figure 1, is consistent with what is expected of a multicomponent hygroscopic aerosol particle. The particle begins to deliquesce at low RH because of the presence of some calcium and magnesium salts of low deliquescence points. However, as RH continues to increase, many of the other salts present begin to dissolve until at about 74% RH, all of the remaining NaCl dissolves and the particle becomes a homogeneous droplet. As RH decreases, the droplet evaporates to become a supersaturated metastable solution until efflorescence suddenly takes place at ~45% RH, similar to a pure NaCl solution droplet. However, like $MgSO_4$ and $MgCl_2$ particles, sea salt aerosol particles do not become completely dry. Some 5-10 wt% residual water is always found to be present in the solid particles.

3.2. Water Activity

Single-particle levitation experiments provide a source of water activity data over a wide concentration range not accessible in isopiestic measurements with bulk solutions. Thus in recent years, water activity measurements have been made with single-salt solution droplets [*Richardson and Spann*, 1984; *Richardson and Kurtz*, 1984; *Tang et al.*, 1986; *Cohen et al.*, 1987a; *Tang and Munkelwitz*, 1994a] and with mixed-salt solution droplets [*Cohen et al.*, 1987b; *Chan et al.*, 1992; *Tang and Munkelwitz*, 1993; *Kim et al.*, 1994; *Tang*, 1997]. In earlier isopiestic solution studies, *Fabuss and Korosi* [1965] reported water activity data of seawater up to 10 wt% of total solids, and *Rush and Johnson* [1966] reported osmotic coefficients of synthetic seawater solutions up to 26 wt% of total solutes. The present work extends the literature solution data to supersaturation up to 46 wt% total solutes.

In Figure 2 the literature water activity data of seawater solutions (both open and solid squares) are plotted as a function

Table 1. Relative Concentrations and Ionic Refractions of Major Ions in Standard Sea Water

Ions	Ionic Ratio	Ionic Refraction
Na^+	1.0*	0.86
Mg^{++}	0.1139	0.03
Ca^{++}	0.0217	1.93
K^+	0.0212	3.21
Cl^-	1.1656	8.09
$SO_4^=$	0.060	13.44

*Na^+ is taken as the reference ion.

of solute weight percent. The solid curve represents the NaCl solution droplet data reported previously [*Tang et al.*, 1986; *Tang*, 1996]. The Long Island seawater data obtained in this work are shown in Figure 2 as open circles. The Atlantic Ocean seawater data, already shown in Figure 1, are in fact in very good agreement with the Long Island seawater data and hence are not shown here again in order not to overcrowd the plot. It is clear that since NaCl constitutes about 80 mol % of total sea salts, the differences in water activity between NaCl solutions and seawater solutions are not appreciable, especially at high concentrations where the differences become almost negligible.

Following previous work [*Tang and Munkelwitz*, 1994a], a polynomial of degree i in the form of

$$a_w = 1.0 + \sum C_i x^i \quad (1)$$

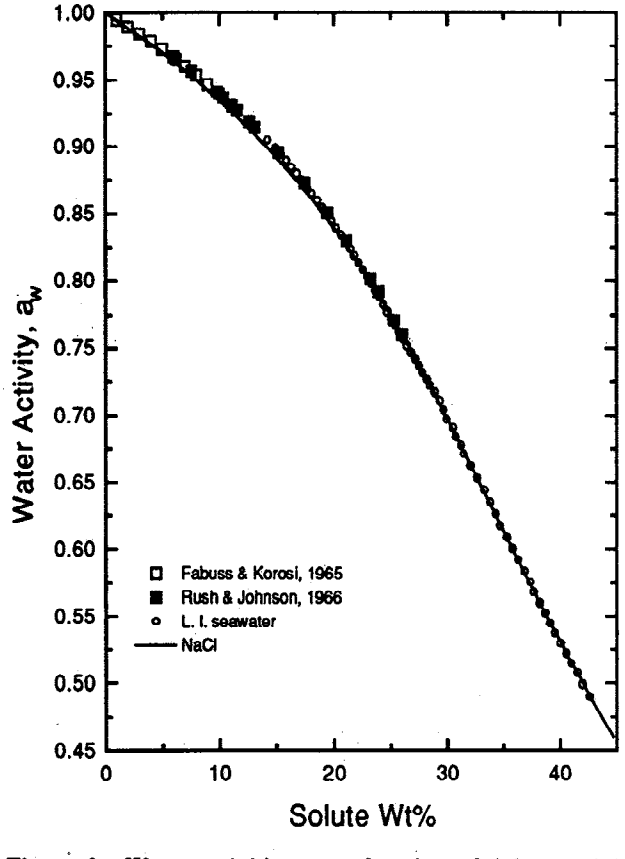

Figure 2. Water activities as a function of solute weight percent for both synthetic and natural sea salt solutions. The solid curve is NaCl solution droplet data shown as reference.

is used to represent the best fit curve of water activity a_w in terms of x, the solute wt%. Here, all water activity data including the two sets of the literature solution data cited above and the droplet evaporation data of seawater samples from both Long Island Sound and Atlantic Ocean are used. The coefficients C_i derived from these data are given in Table 2. In addition, evaporation measurements were made with suspended single $MgSO_4$ and $MgCl_2$ solution droplets. The water activity data obtained for these two systems are each best-fitted with a polynomial, and the appropriate coefficients are given in Table 2. Water activity data of NaCl and Na_2SO_4 solution droplets, which have been published elsewhere [*Tang and Munkelwitz*, 1994a], are also given in Table 2 for completeness. These Mg and Na salts are major constituents of the sea salts that are considered in marine aerosol growth and light-scattering models.

3.3. Density and Molal Refraction

In addition to measuring the weight changes of a single particle, in each experiment the intensity of light scattered from a droplet is continuously monitored at 90° to the incident laser beam illuminating the particle. Typical light scattering as a function of weight percent is shown in Figure 3a for a Long Island seawater droplet and again in Figure 4a for an Atlantic Ocean seawater droplet. Both plots reveal in great details the Mie scattering resonances that occur in a nonabsorbing solution droplet. As RH decreases, the droplet loses water and the nonvolatile solutes become more concentrated. Consequently, the density and refractive index of the droplet are continuously changing with solute weight percent.

Since the solute concentration in an evaporating droplet is precisely known at any time from the dc measurement, it is possible to deduce the density and refractive index simultaneously from the droplet light-scattering diagram by Mie theory. The computational method has been described elsewhere [*Tang and Munkelwitz*, 1991]. It has also been shown previously [*Tang and Munkelwitz*, 1991, 1994a; *Tang*, 1997] that the partial molal refraction approach proposed by *Stelson* [1990] for undersaturated electrolyte solutions is equally applicable to supersaturated solutions of both single and mixed salts. Here we extend the approach to sea salt solutions for which only the ionic compositions, but not the molecular forms of the solutes, are known.

Table 2. Summary of Polynomial Coefficients for Water Activities and Densities

	Seawater	NaCl	Na_2SO_4	$MgCl_2$	$MgSO_4$
x%	0-46	0-45	0-40	0-42	0-50
C_1	-5.872(-3)*	-6.366(-3)	-3.55(-3)	-5.623(-3)	-2.959(-3)
C_2	1.24(-4)	8.624(-5)	9.63(-5)	2.39(-5)	4.495(-4)
C_3	-1.688(-5)	-1.158(-5)	-2.97(-6)	-2.085(-5)	-4.982(-5)
C_4	3.105(-7)	1.518(-7)		2.677(-7)	2.266(-6)
C_5	-1.44(-9)				-5.063(-8)
C_6					4.09(-10)
A_1	7.93(-3)	7.41(-3)	8.871(-3)	8.127(-3)	1.00(-2)
A_2	-4.28(-5)	-3.741(-5)	3.195(-5)	1.237(-5)	3.977(-5)
A_3	2.52(-6)	2.252(-6)	2.28(-7)	5.585(-7)	5.904(-7)
A_4	-2.35(-8)	-2.06(-8)			

* Read -5.872(-3) as -5.872×10^{-3}

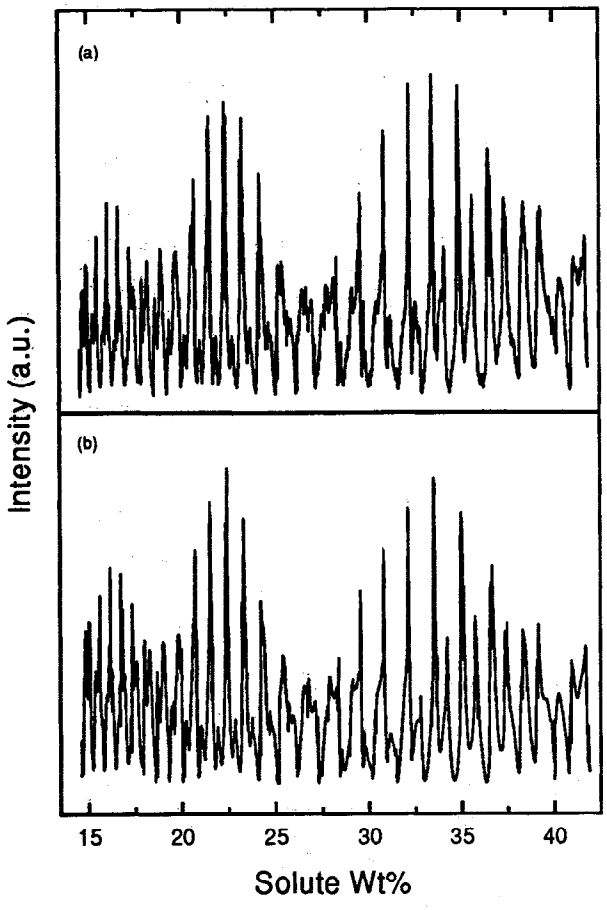

Figure 3. Light-scattering diagram (a. u., arbitrary unit) of an evaporating Long Island Sound seawater droplet: (a) measurement, (b) Mie computation.

By definition, the molal refraction of either a pure substance or a homogeneous mixture of molal volume V and refractive index n is given by [*Moelwyn-Hughes*, 1961]

$$R=\frac{V(n^2-1)}{(n^2+2)} \tag{2}$$

Since the standard seawater is made up of a complex composition of ions, it is necessary to construct an average partial refraction for total solute ions, R_2, such that in combination with the partial refraction of the solvent, R_1, the molal refraction of the droplet may be defined as

$$R=y_1R_1+y_2R_2 \tag{3}$$

where y_1 and y_2 are mole fractions of the solvent water and total solute ions, respectively. The molal volume in (2) is given by

$$V=\frac{1}{d}(y_1M_1+y_2M_2) \tag{4}$$

where d is the density of the solution, and M_1 is the molecular weight of the solvent and M_2 is the average ionic weight of the solute ions. Based on the ion composition of the standard seawater, as given in Table 1, M_2 is evaluated as 31.3.

The average partial refraction of the solute ions is the sum of the partial ionic refractions of all ions weighted by molal concentrations. Table 1 lists the partial ionic refractions of some representative ions in seawater. These values have been validated for all concentrations, using the droplet evaporation method. Based on the ion composition of the standard seawater, R_2 is evaluated as 4.66. R_1 is taken as 3.717 for water. The solution density is expressed by the polynomial

$$d=0.9971+\sum A_i x^i \tag{5}$$

where x is weight percent of total solutes and A_i is the coefficient of the ith term.

Using $M_2=31.3$ and $R_2=4.66$ for the standard seawater, Mie calculations were performed to obtain the solution density as a function of concentration that would produce a scattering diagram in close agreement with the measurement. The results shown in Figures 3b and 4b represent the best of such computations when compared with the corresponding measurements shown in Figures 3a and 4a, respectively. The polynomial coefficients deduced for the density of seawater, according to (5), are given in Table 2. Polynomial coefficients are also obtained for $MgSO_4$ and $MgCl_2$ solution droplets and given in Table 2. Others are taken from data published elsewhere [*Tang and Munkelwitz*, 1994a; *Tang*, 1996].

There are several combination rules proposed for predicting the density of a multicomponent solution from binary data [*Teng*

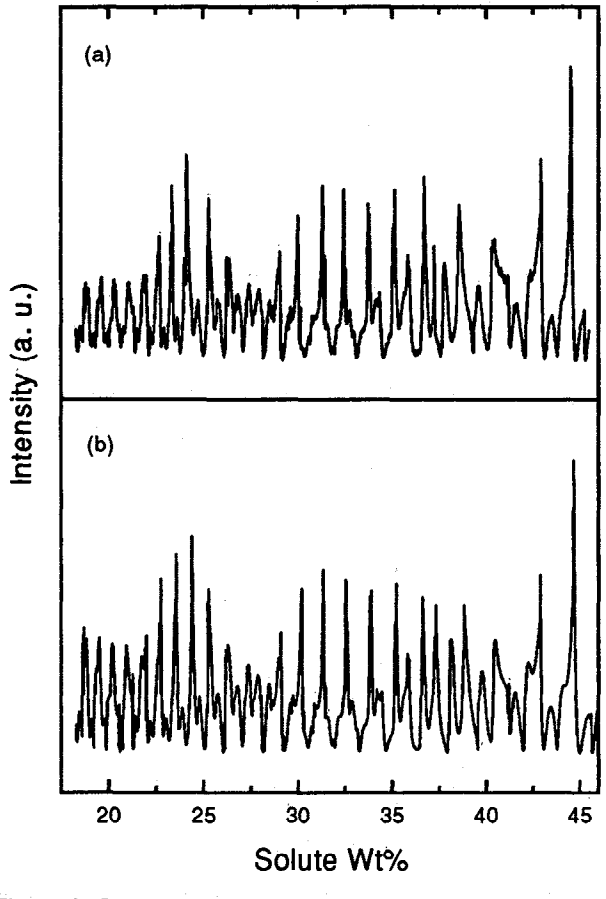

Figure 4. Light-scattering diagram of an evaporating Atlantic Ocean seawater droplet: (a) measurement, (b) Mie computation.

and Lenzi, 1975; *Teng et al.*, 1976]. For most of the mixed-salt systems of atmospheric interest, the following simple volume additivity rule was found to be adequate [*Tang*, 1997]:

$$\frac{1}{d}=\Sigma\frac{w_{oj}}{d_{oj}} \tag{6}$$

where d is the solution density at x wt% of total solutes, d_{oj} is the density of binary solution at x wt% of solute j, and w_{oj} is the weight fraction of solute j present in the total dry salts. However, all predictive methods require that the molecular forms of the solutes be known a priori. To simplify the composition of sea salts, a three-component system (NaCl, Na_2SO_4, and $MgCl_2$) is chosen to represent the four most abundant ions in the normal seawater. Thus the molal composition given in the external mixture (EM) column 1 in Table 3 is taken to represent the freshly formed sea salt particles. This composition gives the same ionic ratios for Na^+, Mg^{++}, and $SO_4^=$ as in seawater but gives a slightly smaller Cl^-/Na^+ ratio as a result of omitting all other ions which are minor components in seawater.

Taking EM 1 as the surrogate sea salts and using (6), the predicted solution density as a function of solute weight percent is computed and plotted as the solid curve in Figure 5. For comparison, the binary solution densities for NaCl, Na_2SO_4, and $MgCl_2$ are also plotted in Figure 5 as dashed curves. The densities deduced from light-scattering measurements of seawater droplet evaporation are shown as open points in Figure 5. The solid points represent the concentrated seawater data reported by *Fabuss et al.* [1966]. The agreement between the predicted and measured densities is excellent.

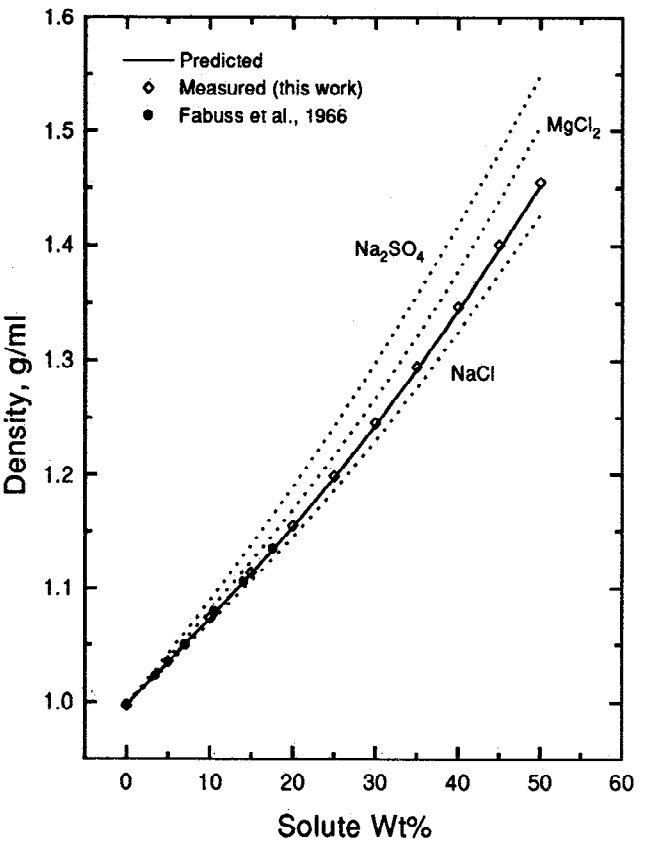

Figure 5. Comparison between normal seawater densities deduced from light-scattering measurements and densities predicted by the volume additivity rule based on the solute composition EM 1. Dotted curves are density data for solutions of NaCl, $MgCl_2$, and Na_2SO_4, which are components used in the prediction. Some limited literature density data for normal seawater concentrates [Fabuss et al., 1966] are also given.

4. Light-Scattering Properties

The thermodynamic and optical data obtained for the sea salt particles allow a comparison to be made of the light-scattering properties between external and internal mixtures for marine aerosols. The method of computing aerosol scattering coefficients as a function of RH has been described elsewhere [*Tang*, 1996]. Briefly, the scattering coefficient, b_{sca}, for an aerosol of given size distribution, $f(D)$, with respect to diameter D may be computed, using the following equation:

$$b_{sca}=\int_0^\infty \pi(D/2)^2 Q_{sca}(\alpha,n)Nf(D)dD \tag{7}$$

where α, the size parameter, is equal to $\pi D/\lambda$. N is particle number concentration, and $Q_{sca}(\alpha,n)$ is the single-particle scattering efficiency factor for given α, wavelength λ, and refractive index n. The wavelength, $\lambda = 0.58$ μm, is chosen as recommended by *Presle and Horvath* [1978] to give the maximum perception of an object under daylight conditions. At this wavelength, there is negligible absorption by either salts or their aqueous solutions and therefore, b_{sca} is equal to the extinction coefficient b_{ext}.

Table 3. External Mixtures Selected to Simulate Sea Salt Aerosols

Salt	EM 1	EM 2	EM 3	EM 4
NaCl	0.835	0.280	0.407	0.517
$MgCl_2$	0.108	0.160	0.074	---
Na_2SO_4	0.057	0.560	0.445	0.346
$MgSO_4$	---	---	0.074	0.137
Cl^-/Na^+	1.108	0.428	0.428	0.428
Mg^{++}/Na^+	0.114	0.114	0.114	0.114
$SO_4^=/Na^+$	0.060	0.40	0.40	0.40

Throughout this study, a constant dry salt loading of 1 μg per m^3 of air is employed as the basis of computation. Thus, b_{sca} has the unit, km^{-1} /(μg /m^3). The dry salt aerosol is assumed to have a lognormal size distribution with count median diameter D_g and geometric standard deviation σ_g. The particle number distribution used in this and previous [*Tang*, 1996] studies facilitates light-scattering computations for particles undergoing growth and evaporation in a changing humidity environment, which is the main interest of these studies.

The humidity effect on the scattering coefficients of a freshly formed sea salt aerosol is shown in Figure 6 as open points. The dry salt aerosol particles are assumed to have a lognormal size distribution ($D_g = 0.3$ μm, $\sigma_g = 1.5$), chosen not as a representation of the actual marine aerosol size distribution, but rather as a convenience for computation and comparison with previous studies. The Kelvin effect due to droplet surface tension is also neglected. Since the computation is based on the water activity and density data obtained for seawater droplets as described above, the results represent the light-scattering properties of the fresh sea salt aerosol as an internal mixture.

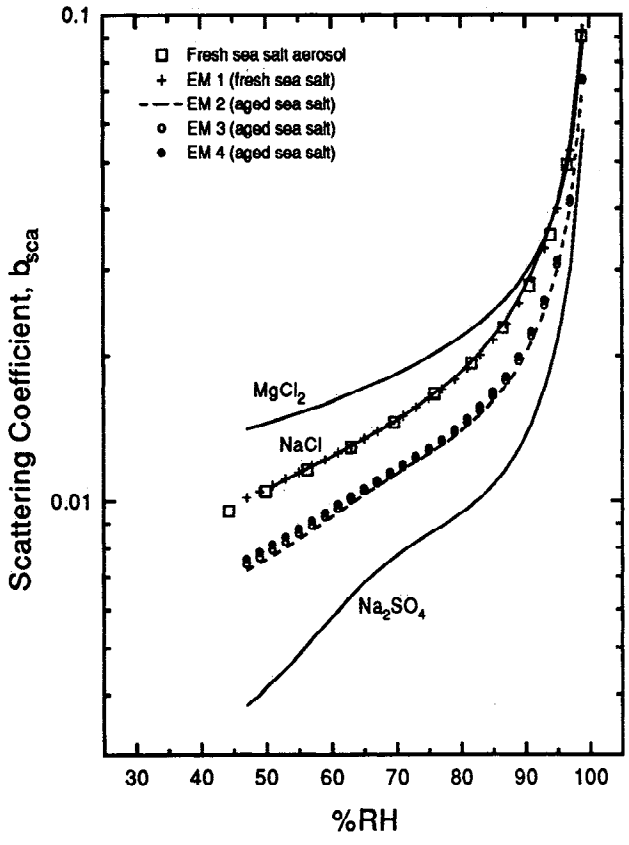

Figure 6. Comparison of light-scattering coefficients calculated for both freshly produced and aged sea salt aerosols of various compositions. Solid curves are for pure component aerosols as designated. Computations are performed for lognormal parameters (D_g = 0.3 μm, σ_g = 1.5) and for dry salt mass 1 μg/m^3 air.

For comparison, computations are performed for component aerosols NaCl, Na_2SO_4, and $MgCl_2$ using the appropriate binary solution data, and the results are plotted in Figure 6 as the individually designated solid curves. It is immediately clear that the light-scattering properties of the seawater aerosol are strikingly close to those of the NaCl aerosol. Scattering coefficients are then calculated for EM 1 approximating the composition of the seawater aerosol, and the results are again plotted as crosses in Figure 6 . It is seen that in agreement with previous findings [*Tang*, 1997], the light-scattering properties of an internally mixed salt aerosol (seawater) can be well approximated by those of an appropriate external mixture (EM 1).

In aged sea salt particles, chemical reactions with gaseous reactants may lead to drastic changes in the elemental ratios. For example, reactions with H_2SO_4 may release HCl from the particle, resulting in low Cl^-/Na^+ and high $SO_4^=/Na^+$. The light-scattering properties of aged sea salt aerosols may thus be different. Taking $SO_4^=/Na^+$ = 0.4 [*McInnes et al.*, 1994], which represents a substantial change from the normal seawater value of 0.06, and letting Mg^{++}/Na^+ remain at the normal seawater value of 0.1139, one can construct a variety of molecular compositions to represent the aerosol. Three such compositions, given in Table 3 as EM 2, EM 3, and EM 4 are designed so as to consider Mg present in the aerosol as $MgCl_2$, $MgCl_2$+$MgSO_4$, and $MgSO_4$, respectively. The Cl^-/Na^+ is 0.428 for all three mixtures, which is substantially less than the value for the normal seawater, thus simulating a loss of Cl in aged marine aerosols. The light-scattering properties of these three externally mixed-salt aerosols are calculated, and the results are again plotted in Figure 6. It is seen that all three sets of points fall closely together in a narrow strip, indicating that as long as the elemental ratios remain unchanged, the molecular composition makes little difference in determining the light-scattering properties of a mixed-salt aerosol. Furthermore, aged sea salt aerosols seem to scatter light less efficiently per unit mass due to Cl losses. This result is true only for the condition that the aged aerosol maintains the same size distribution and mass as those of the starting sea salt aerosol. In reality, however, as chemical reactions and atmospheric mixing proceed, both the aerosol mass and the size distribution will change accordingly. A complete aerosol model, which is not intended in this study, must also take into acount such changes.

5. Conclusions

Water activity, density, and refractive index data at 25°C are presented for sea salt solution droplets over a wide concentration range pertinent to the atmospheric conditions. Thermodynamic and optical data are also given for binary solution droplets containing NaCl, Na_2SO_4, $MgCl_2$, or $MgSO_4$ as the solute. These four inorganic salts are chosen to approximate the compositions of both freshly formed and aged sea salt aerosols of atmospheric interest. It is shown that the light-scattering properties of the sea salt aerosols, be it freshly formed or aged, may be adequately modeled by the external mixtures composed of these four salts. For a given dry particle size distribution, the freshly formed sea salt aerosol scatters light as efficiently per unit mass as the NaCl aerosol.

Along with the inorganic salts, a variety of organic materials may exist as minor contents in marine aerosols. Marine derived alcohols, sterols, and fatty acids are expected on the surfaces of sea salt particles [*Finlayson-Pitts and Pitts*, 1986]. Recent field experiments also show that water-soluble organics may significantly contribute to ambient cloud condensation nuclei [*Novakov and Penner*, 1993]. The effects of both adsorbed and water-soluble organics on the optical and thermodynamic properties of atmospheric aerosols including marine aerosols have yet to be investigated.

Acknowledgments. This research was performed under the auspices of the U.S. Department of Energy under Contract No. DE-AC02-76CH00016.

References

Chameides, W. L., and A. W. Stelson, Aqueous-phase chemical processes in deliquescent sea salt aerosols: A mechanism that couples the atmospheric cycles of S and sea salt, *J. Geophys. Res., 97*, 20,525-20,580, 1992.

Chan, C. K., R. C. Flagan, and J. H. Seinfeld, Water activities of NH_4NO_3/$(NH_4)_2SO_4$ solutions, *Atmos. Environ.,Part A, 26*, 1661-1673, 1992.

Charlson, R. J., J. Langner, H. Rodhe, C. B. Leovy, and S. G. Warren, Perturbation of northern hemisphere radiative balance by backscattering from anthropogenic sulfate aerosols. *Tellus, Ser. B, 43*, 152-163, 1991.

Charlson, R. J., S. E. Schwartz, J. M. Hales, R. D. Cess, J. A. Coakley Jr., J. E. Hansen, and D. J. Hofmann, Climate

forcing by anthropogenic aerosols. *Science, 255*, 423-430, 1992.

Cohen, M. D., R. C. Flagan, and J. H. Seinfeld, Studies of concentrated electrolyte solutions using the electrodynamic balance, 1, Water activities for single electrolyte solutions, *J. Phys. Chem., 91*, 4563-4574, 1987a.

Cohen, M. D., R. C. Flagan, and J. H. Seinfeld, Studies of concentrated electrolyte solutions using the electrodynamic balance, 2, Water activities for mixed-electrolyte solutions, *J. Phys. Chem., 91*, 4575-4582, 1987b.

Duce, R. A., On the source of gaseous chlorine in the marine atmosphere, *J. Geophys. Res., 74*, 4597-4599, 1969.

Fabuss, B. M., and A. Korosi, Thermophysical Properties of Saline Water Systems, *Rep. MRB 6026F*, Table 27, Monsanto, Everett, Mass., 1965.

Fabuss, B. M., A. Korosi, and A. K. M. Shamsul Huq, Density of binary and ternary aqueous solutions of NaCl, Na_2SO_4, and $MgSO_4$, of sea waters and sea water concentrates. *J. Chem. Eng. Data, 11*, 325-331, 1966.

Finlayson-Pitts, B. J., and J. N. Pitts Jr., *Atmospheric Chemistry: Fundamentals and Experimental Techniques*, John Wiley, New York, 1986.

Finlayson-Pitts, B. J., M. J. Ezell, and J. N. Pitts Jr., Formation of chemically active chlorine compounds by reactions of atmospheric NaCl particles with gaseous N_2O_5 and $ClNO_2$, *Nature, 337*, 241-244, 1989.

Fitzgerald, J. W., Marine aerosols: A review, *Atmos. Environ., Part A, 25*, 533-545, 1991.

Kiehl, J. T., and B. P. Briegleb, The relative roles of sulfate aerosols and greenhouse gases in climate forcing, *Science, 260*, 311-314, 1993.

Kim, Y. P., B. K.-L. Pun, C. K. Chan, R. C. Flagan, and J. H. Seinfeld, Determination of water activity in ammonium sulfate and sulfuric acid mixtures using levitated single particles, *Aerosol Sci. Technol., 20*, 275-284, 1994.

McInnes, L. M., D. S. Covert, P. K. Quinn, and M. S. Germani, Measurements of chloride depletion and sulfur enrichment in individual sea salt particles collected from the remote marine boundary layer, *J. Geophys. Res., 99*, 8257-8268, 1994.

Moelwyn-Hughes, E. A. *Physical Chemistry*, 2nd rev. ed., Pergamon, Tarrytown, New York, 1961.

Novakov, T., and J. E. Penner, Large contribution of organic aerosols to cloud-condensation-nuclei concentrations, *Nature, 365*, 823-826, 1993.

Orr, C., Jr., F. K. Hurd, and W. J. Corbett, Aerosol size and relative humidity, *J. Colloid Sci. 13*, 472-482, 1958.

Presle, G., and H. Horvath, Visibility in turbid media with colored illumination. *Atmos. Environ. 12*, 2455-2459, 1978.

Richardson, C. B., and C. A. Kurtz, A novel isopiestic measurement of water activity in concentrated and supersaturated lithium halide solutions, *J. Am. Chem. Soc., 106*, 6615-6618, 1984.

Richardson, C. B., and J. F. Spann, Measurement of the water cycle in a levitated ammonium sulfate particle, J. *Aerosol Sci., 15*, 563-571, 1984.

Rush, R. M., and J. S. Johnson, Osmotic coefficients of synthetic sea-water solutions at 25°C, *J. Chem. Eng. Data, 11*, 590-592, 1966.

Stelson, A. W., Urban aerosol refractive index prediction by molar refraction approach, *Environ. Sci. Technol., 24*, 1676-1679, 1990.

Sverdrup, H. V., M. W. Johnson, and R. H. Flemming, *The Ocean*, Prentice-Hall, Englewood Cliffs, New Jersey, 1942.

Tang, I. N., Phase transformation and growth of aerosol particles composed of mixed salts, *J. Aerosol Sci., 7*, 361-371, 1976.

Tang, I. N., The chemical and size effects of hygroscopic aerosols on light scattering coefficients, *J. Geophys. Res., 101*, 19,245-19,250, 1996.

Tang, I. N., Thermodynamic and optical properties of mixed-salt aerosols of atmospheric importance, *J. Geophys. Res., 102*, 1883-1893, 1997.

Tang, I. N., and H. R. Munkelwitz, Simultaneous determination of refractive index and density of an evaporating aqueous solution droplet, *Aerosol Sci. Technol., 15*, 201-207, 1991.

Tang, I. N., and H. R. Munkelwitz, Composition and temperature dependence of the deliquescence properties of hygroscopic aerosols. *Atmos. Environ., Part A, 27*, 467-473, 1993.

Tang, I. N., and H. R. Munkelwitz, Water activities, densities, and refractive indices of aqueous sulfates and sodium nitrate droplets of atmospheric importance, *J. Geophys. Res., 99*, 18,801-18,808, 1994a.

Tang, I. N., and H. R. Munkelwitz, Aerosol phase transformation and growth in the atmosphere, *J. Appl. Meteorol., 33*, 792-796, 1994b.

Tang, I. N., H. R. Munkelwitz, and N. Wang, Water activity measurements with single suspended droplets: The NaCl-H_2O and KCl-H_2O systems, *J. Colloid Interface Sci., 14*, 409-415, 1986.

Teng, T.-T., and F. Lenzi, Density prediction of multicomponent aqueous solutions from binary data. *Can. J. Chem. Eng., 53*, 673-676, 1975.

Teng, T.-T., J. Sanster, and F. Lenzi, Additivity rules for the prediction of the density of aqueous solutions containing mixed-type solutes, *Can. J. Chem. Eng., 54*, 600-605, 1976.

K.H. Fung and I.N. Tang, Environmental Chemistry Division, Department of Applied Science, Building 815, Brookhaven National Laboratory, Upton, NY 11973-5000. (e-mail: fung@bnl.gov; tang@bnl.gov)

A.C. Tridico, 1015 North Stuart Street, #317, Arlington, VA 22201.

(Received April 1, 1997; revised June 9, 1997;
accepted June 18, 1997.)